BACHELOR THESIS

Extending the Software Environment of the qBounce Platform

Institute of Atomic and Subatomic Physics
University of Technology, Vienna

under the supervision of

Univ.Prof. Dr. Hartmut Abele

by

Nikolaus Huber
Matr. Nr.: 1225274

June, 2017

Abstract

The *q*Bounce experiments are a collection of tests aiming for a wider understanding of the nature of gravity within micron interaction ranges. In order to allow the detection of socalled ultracold neutrons a new kind of neutron detector has been established at the Atominstitut, which is able to detect neutrons with low velocities with an ultra-low background. Therefor a neutron interacts with a boron layer, which emits Li and α particles at verious energy levels. These can be measured with such a detector. Previous tests have shown that the results suffer from fluctuations in the environmental parameters like pressure and flow rates of the $AgCO_2$ gas flowing through the detector, resulting in a energy drift of the overall spectrum data. The aim of this bachelor thesis is to help introducing a reliable form of continuous measurement of these parameters, including the establishment of a software environment for tracking and the interpretation of the connection between the parameters and the shift of the resulting neutron spectrum.

Zusammenfassung

Im Rahmen der *q*Bounce Experimente werden Tests zur Untersuchung des Newton'schen Gravitationsgesetzes auf Längenskalen im Mikrometerbereich durchgeführt. Am Atominstitut Wien wurde ein spezieller Detektor entwickelt, welcher die für diese Tests verwendeten ultrakalten Neutronen messen kann. In diesem regen durch eine Borschicht durchtretende Neutronen Boratome zum Zerfall in Li und α Teilchen an, deren unterschiedliche Energien mit diesem Detektor gemessen werden können. Zuvor durchgeführte Messungen haben gezeigt, dass das aufgenommene Energiespektrum durch Variationen des Gasdrucks und der Durchflussrate des $AgCO_2$ Gases durch den Detektor beeinflusst wird. Ziel dieser Bachelorarbeit ist es, eine Software zur durchgängigen Messung dieser Parameter zu erstellen und dadurch deren Verbindung mit dem Drift des Energiespektrums zu untersuchen.

Acknowledgement

I wish to express my sincere thank you to Martin Thalhammer. Without his continuous assistance and supervision this thesis would have never been accomplished. I would like to thank you very much for your support and understanding throughout this project.

Furthermore I would like to express my gratitude to all staff members of the Atominstitut who were involved in this thesis, especially all members of the *q*Bounce research group, who always assisted me when I encountered any problems.

Last but not least, I want to thank Andrzej Pelczar, supervisor of the Electronics Department, for his invaluable support with the electronic circuits used in this project.

Contents

1 Introduction

The *q*BOUNCE collaboration investigates Newton's inverse square law of gravity on a micron interaction range with a quantum interference technique. To gather new insight on the way gravity works on small length scales physicists at the Atominstitut (ATI) use ultracold neutrons (UCNs) as a testparticle. For that purpose several different experiments are performed.

UCNs are characterised as having kinetic energies so low, that their corresponding de Broglie wavelength is larger than the average distances of atoms in matter. Therefore, they are reflected on surfaces under every angle of incidence, resulting from the appropriate Fermi-potential [1].

Even though neutral atoms could be used for this type of experiments due to their lack of electrical charge, neutrons are considered more appropriate for gravitational experiments as their polarisability is much lower. Nevertheless, electromagnetic shielding is important since the magnetic momentum of neutrons stills accounts to $\mu_n = (-0.96623650 \pm 0.00000023) \cdot 10^{-26} \cdot JT^{-1}$ [2].

There have been a lot of different experiments aiming for a proof of Newton's law of gravity, resulting in its unquestionable acceptance among scientist. However, there are remaining parts on the length scale that still need investigation. Deviations from predicted results on micron length scales may open the opportunity for new theories for gravitation, probably also leading to further understanding of concepts like dark energy or dark matter [3].

One of the current candidates for dark matter are chameleon particles [4, 5]. These hypothetical particles would result in a quantum field, coupling to matter in such a way, that whenever the ambient energy density is high, it vanishes. This would explain, for example, why these fields have no interaction with the orbits of planets, but could still result in an enormous force when applied to bigger objects in our universe, like galaxies, where the density of matter is low.

Another notable hypothesis that would profit from variances in Newton's law are certain kinds of String theories. As these theories are formulated in a mathematical space of at least 10 dimensions the question arises to where these extra dimensions are located since we only see the results of 3 of them. Therefore physicists came up with the idea of coiled up dimensions. These would not affect objects laying within spacetime when the distance of interaction is large enough, but may still cause gravitational deviations when the range of interaction enters the radius of the coiled up dimensions which could be in the micron length scale [6].

For all of the experiments within the qBOUNCE environment, a low background neutron counter is needed in order to measure the transmission of low neutron count rates. Part of this bachelor thesis was to establish a software integration of the neutron detector into a pre-existing LabVIEW environment. Previous versions of this detectors have been used at the ATI and at the Institute Laue Langevin (ILL). As the results from these test have suffered from variations on the gas pressure and flow rate of the $AgCO_2$ gas flowing through the detector, the need for a software based tracking system of said environmental parameters has arisen. Within the work of this bachelor thesis, sensors have been installed into the detector setup and a software environment has been established in order to allow the continuous recording of pressure and flow rates in the detector.

2 The Detector System

Within the qBOUNCE experiments a low background neutron counter has to be used, in order to track the UCNs which went through the different experimental setups.

2.1 The Boron Converter

In order to detect UCNs a converter material has to be used. Within the qBOUNCE experiments, ^{10}B is used as a neutron converter, as it has a large absorption cross section for UCNs. After a neutron gets captured, a B Atom decays into alpha and Li particles. One can distinguish between two different channels with different probabilities and energy levels of the resulting ions:

$$\text{I:} \quad n + {}^{10}B \quad \rightarrow \quad \alpha + {}^{7}Li^{*} \quad \rightarrow \quad \alpha + {}^{7}Li^{3+} + \gamma\,(0.48\,\text{MeV}) + 2.31\,\text{MeV} \tag{2.1}$$

$$\text{II:} \quad n + {}^{10}B \quad \rightarrow \quad \alpha + {}^{7}Li^{3+} + 2.97\,\text{MeV} \tag{2.2}$$

The probability of 2.1 is 94 %, the likelihood of 2.2 is therefore 6 %. Since the kinetic energy of the UCNs is small in comparison to the resulting ions in above given equations, the momenta of the ions is expected to be isotropic [7]. The detection system used only covers the particles emitted on one side of the converter.

The thickness of the the B layer is essential to allow a good balance between neutron absorption rate and ion transmission through the rest of the layer. A thickness of 221 nm has been calculated as an optimum for detecting neutrons with a mean velocity of 6.5 m/s [8].

To detect the emitted ions, a proportional counter is placed behind the boron layer.

2.2 The Proportional Counter

The proportional counter is realised as a cylindrical capacitor. Figure 2.1 shows a schematic side-cut through the detector, illustrating the neutron entrance window (1), which is crafted out of $AlMg_3$ due to its small crosssection [9], the boron layer behind the window (2) which is used as the converter material and the gold coated tungsten filament (3) which functions as the anode of the capacitor. The brass housing serves as the cathode, grounded by a high voltage feed-through. The chamber is flooded with $AgCO_2$ gas with a ratio of 90:10. The Ag gas is used for gas amiplification, the CO_2 gas in order to absorb the gamma quants resulting from the neutron conversion.

The detector is used in flow mode to prevent ageing phenomena, even though it is very difficult to seal the detector chamber tight.

The detector is optimised on low background rates, therefore several adjustments can be seen on the system. First, the window area is restricted to 3 x 110 mm, which covers all relevant neutron paths but allows efficient shielding against other neutron radiation, which could be a problem in nuclear research facilities such as the ILL. Moreover, the high voltage has been adjusted so as to reduce voltage sparks inside the chamber while still allowing sufficient gas amplification. Therefore the anode diameter has been minimised to a diameter of 15 μm and the distance between the wire and the neutron window has been chosen to 12 mm, since the most energetic ion emitted while converting has an average stop range of 9.26 mm. With these adjustments the detector can be used with voltage levels between 350V and 1000 V.

2.3 The Electronics

When an alpha particle reaches the anode, the deposited charge is collected with an RC circuit and converted to a voltage signal by a charge sensitive preamplifier. This signal is increased to a range between 0V and 10V by a main amplifier.

Evolving from previous tests a commercially available preamplifier has replaced a formerly custom constructed one. In this setup, the CR-110 charge sensitive amplifier by Cremat [10] has been used. The signal is further amplified by an Ortec 570 [11] due to its low noise characteristic.

The reading out is performed by an Itech Instruments four-channel analog-to-digital converter (quadADC) [12] with two logic channels. As the neutron beam at ILL is shared between different experimental platforms these channels are used to distinguish between neutron and background time.

Since the neutron beam itself is in fact fluctuated, a beam monitoring system is used to normalise the resulting spectrums.

2.4 Software Based Optimisations

To allow low-noise background sufficient measurements, a few software based optimisations have been introduced into the project. A burst filter is used to remove detector events with a time leg less than a given burst parameter since events with an average count rate of more than $10^{-4}s^{-1}$ are more likely to be noise [13].

2.5 Gas Pressure and Flow Rate Sensors

As previous experiments done by M. Thalhammer have shown a significant shift of the neutron spectrum due to fluctuations of gas pressure and flow rates of the $AgCO_2$ gas in and through the detector, a gas pressure sensor has been inserted into the chamber while flow rate sensors have been put before and after the chamber within the gas supply tubes.

Therefore, three Honeywell Zephyr TM Digital Airflow Sensors [14] have been characterised within the bachelor thesis of P.T. Heistracher [15], showing that even though all sensors were functioning within their promised working range there are significant differences when using these with such low flow rates. The two sensors that showed the most coinciding characteristics where then placed into the experimental setup.

To track the pressure inside the chamber a Honeywell ASDX Series Silicon Pressure Sensor [16] has been inserted into the proportional counter.

All communication with above given sensors is done through the I2C protocol. The connection to the PC system is achieved by an ELV-USB-I2C-Interface [17].

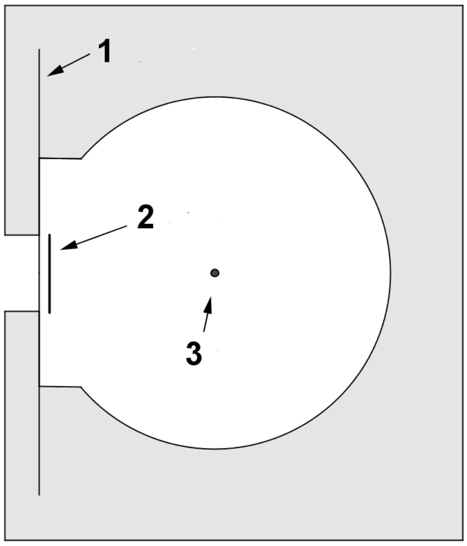

Figure 2.1: Schematic overview of the neutron detector. (1) neutron entrance window, (2) boron layer, (3) tungsten filament.

3 The Software

3.1 Overview

The aim of this bachelor thesis was to create a reliable software system to control the neutron spectrum acquisitonto and to continuously read the data received from the flow and pressure sensors. The overall structure of the software environment is laid out in figure 3.1. All programming is done in LabVIEW [18] wich offers a sophisticated environment for the overall platform control. Coding is done by using LabVIEW's own graphical programming language called *G* which is used by arranging so-called virtual instruments (VI). Every VI consists of two parts, a *Front Panel* and a *Block Diagram*. The Front Panel holds the graphical user interface which allows the user to input data and receive data from the program. The Block Diagram contains the program's logic and all the G code. Data can either be present as user input from the Front Panel, as constants which are hardcoded into the Block Diagram or as output values from other VIs. The program flow is controlled by placing special areas on the Block Diagram which implement structures like *if ... then ... else* or loops known from traditional scripted programming languages. Within these structures there can be any number of so-called SubVIs, which are fully functional LabVIEW programs themself. The input and output fields on the Front Panel can be exposed to the outside of the VI in order to use them as SubVIs in other programs. Every output from a given VI must be connected to either the input of another VI or to an output variable on the Front Panel.

LabVIEW comes with a standard library which offers VIs to accomplish essential programming tasks like accessing files or doing mathematical calculations.

Figure 3.2 illustrates a very simple example of a LabVIEW VI that adds two numbers together. Subfigure (a) shows the Front Panel with two socalled *Numeric Controls* on the left and one *Numeric Indicator* on the right side. When the program is run, LabVIEW adds the two numbers that are present in the *Numeric Controls* and shows the result in the *Numeric Indicator*. Subfigure (b) displays the respective Bock Diagram, where there are indicators for the associated values on the Front Panel. The input values are wired to an arithmetic function that

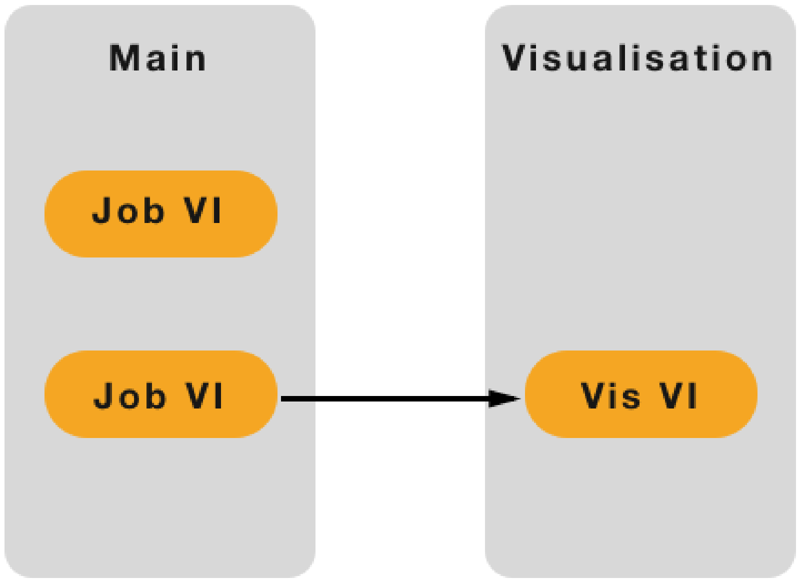

Figure 3.1: Structure of the software project.

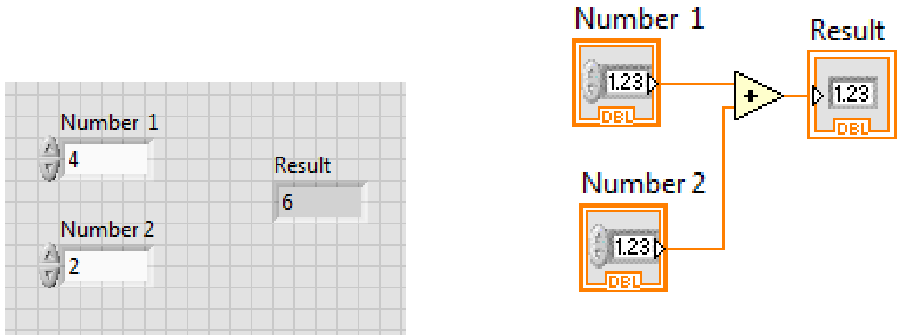

(a) (b)

Figure 3.2: A simple VI in LabVIEW: (a) Front Panel, (b) Block Diagram.

is part of LabVIEW's standard library and the output is wired to the output control. Moreover it is important to notice that any SubVI or function on the Block Diagram waits until there are values on all connected input wires.

Many hardware vendors for different measurement and control systems also offer collections of VIs to access and control their platforms, which is the reason why LabVIEW has been chosen as the background environment for this experiment.

As shown in 3.1 there are essentially two different VIs that are always up and running. The *Main VI* controls the overall project and holds a number of different Job VIs. Every Job VI controls a different part of the hardware platform used for the experiment, the different Job VIs are controled by toggle buttons. When a button for a specific job is pressed the corresponding Job VI is loaded by the LabVIEW runtime environment and if said Job VI offers a visual representation of its data model it is loaded into the *Visualisation VI*.

For this theses two Job VIs have been created. One for the continuous readout of the pressure and flow sensors used within the detector system and one for the control of the neutron spectrum acquisition.

3.2 Detector Control

3.2.1 Requirements

Figure 3.3 represents the overall structure of the detector setup. The detector itself (with an inline preamplifier) is connected to an oscilloscope to offer an on-site verification that the detector is working properly. The detector output is further connected to an Ortec 570 [11], a general purpose spectroscopy amplifier via a 50 Ω termination resistor. The amplified signal is then processed by a quadADC [12], a four channel analog to digital converter by Itech Technologies[1]. As the neutron beam at ILL is shared between different experiments there has to be a way to distinguish neutron from background time within the collected data. Therefor the quadADC offers 2 logical inputs, which can be used to differentiate between time where the neutron beam is directed towards the detector and background time. Itech Technologies also offers a special software called InterWinner [19] which is used to control the quadADC and visualize and save the data collected from it.

[1] www.itech-technologies.com

The task was to create a connection between InterWinner and the Job VI that is utilised to control the detector and also to visualize the spectrum data within the Visualisation VI. Therefor a special program called Decode, written by Martin Thalhammer, has been used to convert the spectrum data from InterWinner's specific binary file format to a general Comma-Separated Values File (CSV).

3.2.2 Software Design

As there is currently no possibility of a direct communication between LabVIEW, InterWinner and Decode another way of interaction had to be found.

InterWinner offers an interface that allows the usage of scripts written in a specific dialect of Virtual Basic Script (VBScript) to control the program. These scripts are called MAKs.

```
1  #language VBScript
2  Sub StartMeasurement
3    main.Hide
4          Dim acq0
5          set acq0 = main.acquisition(0)
6          acq0.Start
7          main.acquisition(1).Start
8          main.acquisition(2).Start
9          main.acquisition(3).Start
10         acq0.SaveAs "L:\3-14-358_test\InterWinner\1-008"
11 End Sub
12 StartMeasurement
```

Listing 3.1: MAK to start a measurement.

Listing 3.1 shows an example for the MAK that is used to start the recording of a new spectrum. In line 2 a subroutine is defined which is than executed in line 12. The command *main.hide* prevents InterWinner from showing it's own graphical user interface, since all output should be forwarded to the Visualisation VI. Lines 4 to 6 set up a new data acquisition and start the measurement. The different *main.acquisition(...)* tokes relate to different input values at the logical input gates of the quadADC. The last line in the subroutine sets up the filename of the spectrum and the path where it is saved.

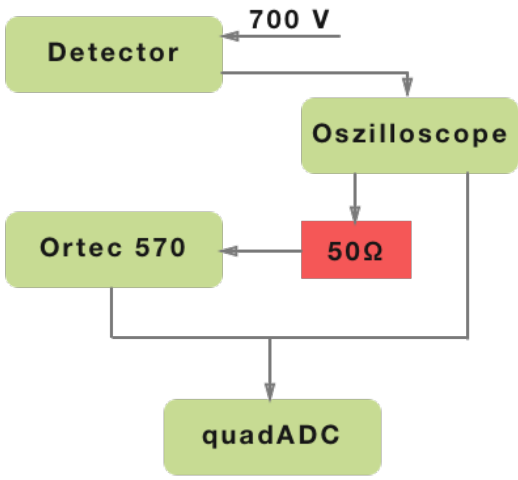

Figure 3.3: Structure of the electric setup.

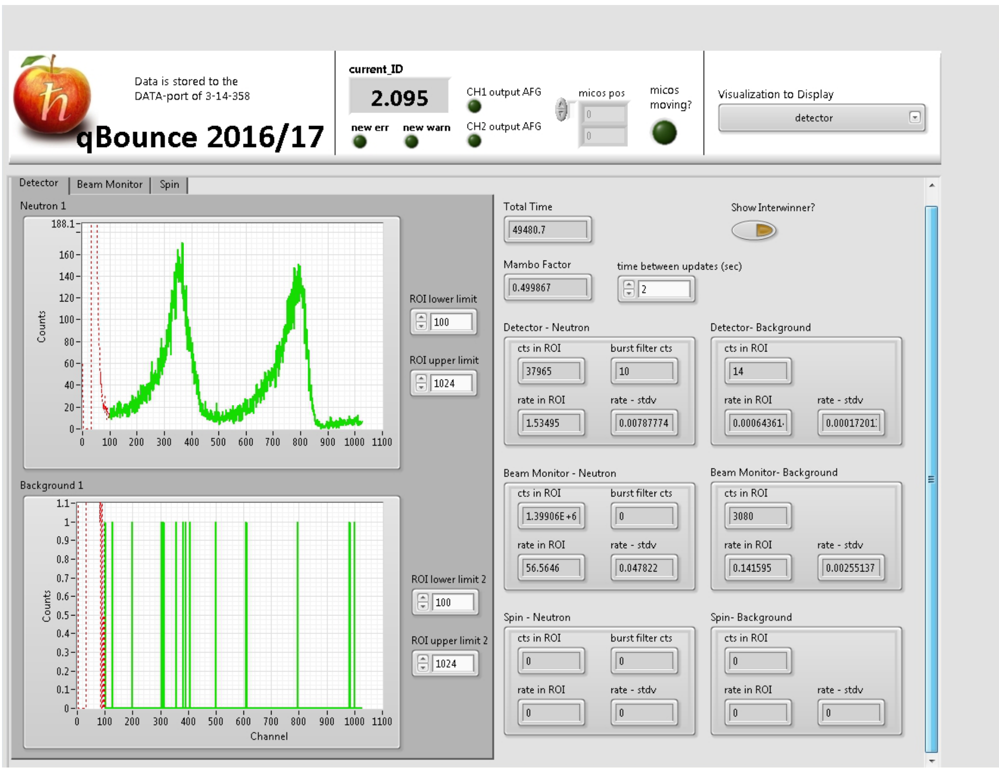

Figure 3.4: The Visualisation VI showing the Front Panel of the Detector Control VI.

Every new measurement gets a unique ID. As this ID increases with every recorded spectrum, the MAK that is used to start a new spectrum acquisition is generated by LabVIEW for every new ID. LabVIEW's standard library provides an interface to the commandline of the operating system, which is used to run the MAK files. The overall connection between LabVIEW and InterWinner thus consists of MAK files, which control InterWinner and are called by LabVIEW via its commandline interface.

LabVIEW currently offers little support in exposing its internal variables to the outside of the program. Therefor the interaction between LabVIEW and Decode has to rely on a common set of plain text files, each containing the value of a controlling variable that both programs have to read out continuously. This involes files with toggle values to stop Decode from running, or files with values to control the conversion rate.

At the beginning of a new measurement LabVIEW sets up InterWinner by calling the respective MAKs. After InterWinner has been initialized LabVIEW generates the set of common interaction files, setting values like the update rate per second or burst filter values. After that LabVIEW starts up Decode by also calling the program through the commandline interface. At the end of the measurement LabVIEW changes the file that holds the on/off toggle value and sets the running variable to false, which causes Decode to halt.

Overall, the design choices made result in a sighlty slower performance, as the continuous readout functions consume more processing power than a direct communication. However as already pointed out, there is currently no possibility to access LabVIEW's variables from outside the program.

Figure 3.4 shows the Front Panel of the Detector Control VI within the Visualisation VI. On the left side it illustrates the spectrum that is currently recorded with the neutron spectrum on the top and the background spectrum on the bottom. On the right side it displays important experimental parameters the like the total time of the measurement, the count rate and the overall counts within the ROI 4.2.

3.3 Detector Sensors

3.3.1 Requirements

Figure 3.5 shows the overall setup for the supply gas for the detector. To ensure that there are no leaks two flow sensors have to be used. Between the flow sensors and the detector itself there is a tube interrupted by a stop and a control valve respectively. The pressure sensor is located within the detector to measure the pressure inside the proportional counter.

As previously done experiments have shown there is a drift in the recorded spectrum according to the pressure of the supply gas within the detector. That is why a continuous record of the pressure has to be kept in addition to the spectrum data.

All communication with the sensors is done via the I2C protocol. This protocol requires two different lines, one for the data and one for the periodic clock signal. The I2C protocol establishes a master/slave architecture with the computer as the master device. Every sensor has a unique address that the master can use to start communicating with it.

As sensors sometimes have to be changed, or a different number of sensors may be desired to be used there has to be a way to isolate this information from the program itself.

3.3.2 Software Design

Since the number and the address of the sensors is not known during coding some form of initialisation file has to be used. The standard file format INI has been chosen for its simplicity and easy integration with LabVIEW. INI files are a collection of assignments in the form of *variable = value*. At the beginning of each measurement LabVIEW parses this INI file and looks for a special variable called *sensors*. Its value contains any number of *sensor cluster values*, a special format to specify a single sensor. Each sensor cluster value contains the address and the name of the sensor, the COM Port of the computer that the I2C controller is connected to, a type indentificator that signals if it is a flow or a pressure sensor, the number of bytes that the sensor sends, and an optional multiplexer (MUX) address, if a MUX is used. An example of the sensors variable could be:

sensors = COM7,51,E004,P,pressure1,4/COM7,93,E005,F,flow1,2

This lets LabVIEW know that there are two sensors connected to the I2C controller at COM7, the first being a pressuresensor *P* named *pressure1* with the address *51* (hexadecimal) and a MUX adress of *E004* (hexadecimal) that sends 4 bytes of data when called by the master device. The second sensor after the forward slash is analysed in the same way.

Through this design it is possible to add any number of pressure and flow sensors in the setup by just adding them to the sensors variable in the INI file, which improves maintainability.

The Job VI that controls the sensors consists of two loops running in parallel mode. One loop is used to read out data from the sensors (read loop) the other for processing (process loop). With each iteration the read loop runs through all the sensors specified in the sensors variable in the INI file and receives the respective amount of bytes. It then generates a cluster variable, containing the sensor data and the type of the sensor which it passes on to a queue data structure shared between the two loops. The process loop takes one cluster from the queue with each iteration and calculates the measurred value by calling sensor specific evaluation functions that are triggered by the type indicator sent with the cluster. The process loop also updates the value on the Visualisation VI and saves it.

As an example, figure 3.6 shows the Sensor VI that runs within the read loop. On the left side there is the input cluster, which is essentially a structured representation of the information gathered from the sensors variable in the INI file. The surrounding grey box is called a *Sequence Structure* with different *Frames*, which ensures that every SubVI in one Frame has finished its processing before moving on to the next frame. In the first Frame, a SubVI called *Init Sensor* is executed, which opens the connection to the COM port. The next Frame contains a *Sensor Write VI* which can set the MUX address of the sensor, if the value of the address given in the INI file is not zero, which is illustrated as the *Comparison Function* before the *True/False Case Structure*. Afer that the *Sensor Write VI* sends the *read command* to the sensor. The *Sensor Read VI* reads the data from the sensor, followed by the *Sensor Close VI* to close the connection. The read out data is put into a cluster together with the name and type identificator from the input cluster.

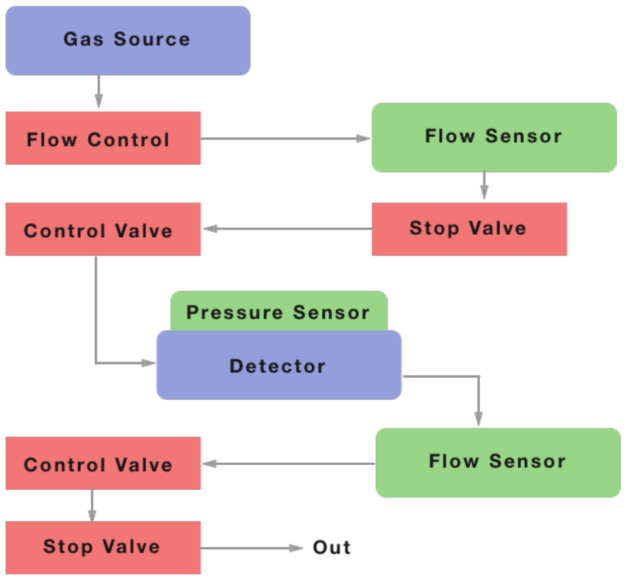

Figure 3.5: Overview of the gas system setup.

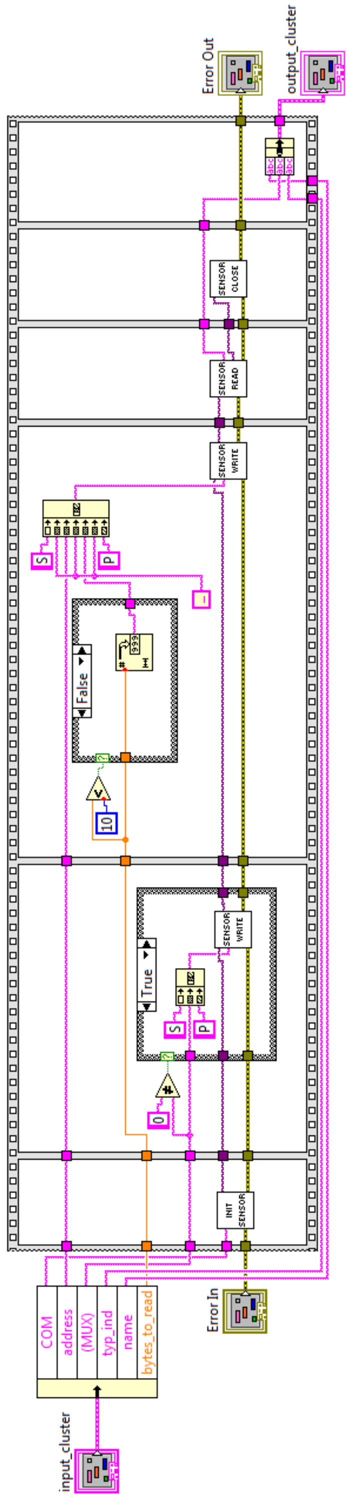

Figure 3.6: The Block Diagram of the Sensor VI.

4 Analysis of Spectrum Data

The neutron spectrum data acquired from the software environment that is laid out in chapter 3 can now be reviewed for a potential connection between the gas pressure in the detector chamber and the drift of said spectrum. The data was collected at the PF-2 testbeam slot at the ILL with varying pressure values inside the detector but with fixed electrical amplification.

4.1 Measurement of Drift

The acquired neutron spectrum shows the intensity (total number of counts) over the channel number of the InterWinner ADC which corresponds to different energies. As shown by equations 2.1 and 2.2 there are two possible ways that a boron atom can decay into α and Li particles with different kinetic energies. Therefore the neutron spectrum illustrates four different peaks, two for the α and two for the Li particles that were produced inside the boron layer. As the likelihood of the two decay channels are different (94 % and 6 %), the intensity of the channel that results in particles with higher energy is considerably lower. In figure 4.1 four different neutron spectra are shown. The two major peaks are the Li particle (at approx. channel number 350) and the α particle (at approx. 750) of decay channel 2.1. The other peaks for decay channel 2.2 are harder to see, the α peak is at approx. channel number 950, the Li peak around channel number 500. Since the particles can be produced at any point within the boron layer, the spectrum also reaches channel number 0, as the resulting decay products must further travel through the remaining layer which causes kinetic energy loss. The fluctuations within the lowest channel numbers result from different noise sources, therefore the data in the lower channels is usually neglected (see chapter 4.2).

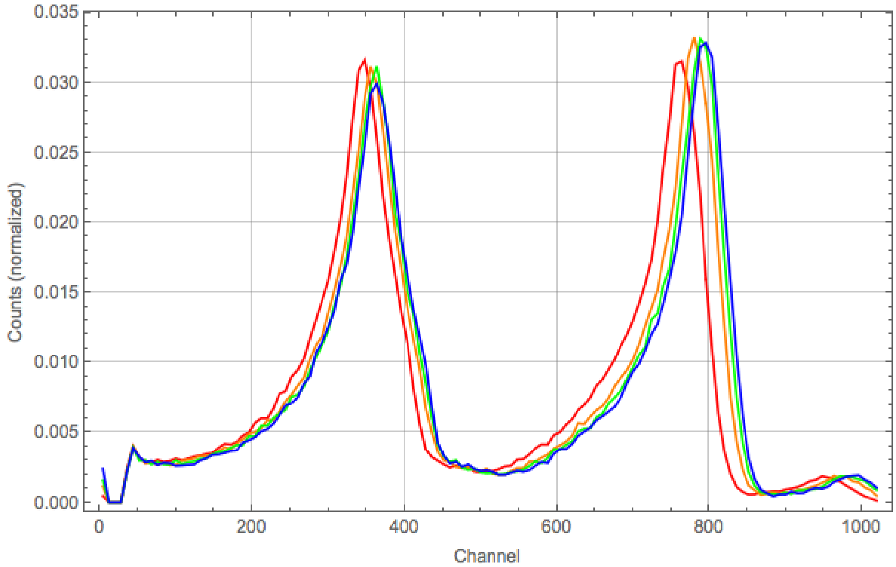

Figure 4.1: Spectral data from different measurements for an approximate mean value of 1010 hPa in the detector. Temporal order of measurements: Red, Orange, Green, Blue.

As can be seen from figure 4.1, several measurements were done for the same value of gas pressure within the detector. There is a noticeable drift of the spectrum even at approximately the same pressure level which must be considered within the error band of the position (see chapter 4.3).

4.2 The Theory Function

In order to allow for a better comparison between the spectra at different gas pressure levels, the obtained data is fitted to a theory function. This function uses results from a computer simulation of the energy loss of α and Li particles travelling through a boron layer. The theory function is presented in depth in [20].

To further improve the fitting process a region of interest (ROI) is defined. It is the smallest possible region, that contains all the spectrum data, or the relevant part of it, while still excluding noise from electrical or other sources. [13]

4.3 Analysis of Drift

In order to allow a comparison between the drift of different spectra, a measurement for this drift has to be defined. Each spectrum is fitted to the theory function introduced in chapter 4.2 with 3 different parameters. Given the theory function $f_{\text{theory}}(x)$ with f_{theory} as the intensity and x as the energy, the spectrum data is fitted to the function $\gamma \cdot f_{\text{theory}}(\alpha \cdot x + \beta)$. The parameter γ scales the spectrum along the ordinate, α along the abscissa and β is an offset. After fitting every spectrum to the theory function a meanvalue $\bar{\beta}$ of the offsets is determined and every spectrum is fitted again to $\gamma \cdot f_{\text{theory}}(\alpha \cdot x + \bar{\beta})$. The resulting parameter α for the abscissa is used to define the overall position of each spectrum.

To allow a better comparison between the spectra at different pressure levels and to eliminate equally distributed errors all α parameters are used relatively to α_{1030} at a pressure value of $1030\,hPa$.

Referring to [21] the error of the pressure value that results from the pressure sensor used in this detector consists of multiple sources. As the detector is kept in a stable temperature environment thermal effects can be neglected. Furthermore the pressure values are used relatively to $1030\,hPa$, therefore all sensor offset and full scale span errors are also irrelevant, leaving only non linearty, sensor hysteresis and pressure non-repeatability, collectively called accuracy, to consider as noticeable error sources. The manufacturer guarantees a total error band of $\pm 2\%$ at a maximum, but since in this case only the accuracy adds to the error this band may be to high. The estimated error band caused by accuracy is stated at $\pm 0.25\%$ of the full span of the sensor. It is important to notice that the negligence of the error resulting from sensor offset and full scale span are only valid because of the use of a relative reference point at $1030\,hPa$, therefore an overall error band up to $\pm 2\%$ must be considered for this value.

If the measurements were perfect all spectra overlaid should result in a single line. The different peaks of the neutron spectra show a good overall alignment, but have varying widths. To estimate the error band of the spectrum position the full width at half maximum for the α and Li peaks of decay channel 2.1 are added together for each spectrum. The difference between the resulting minimum and maximum value of all spectra is taken as the error resulting from the difference in peak widths and the general error in the peak position. For the spectra used for the analysis in this thesis the resulting error is approximately 0.5%.

Another source that adds to the error band of α results from the observation that even if the gas pressure inside the detector chamber is stable there is still a perceivable drift of the spectrum over multiple measurements on the same pressure

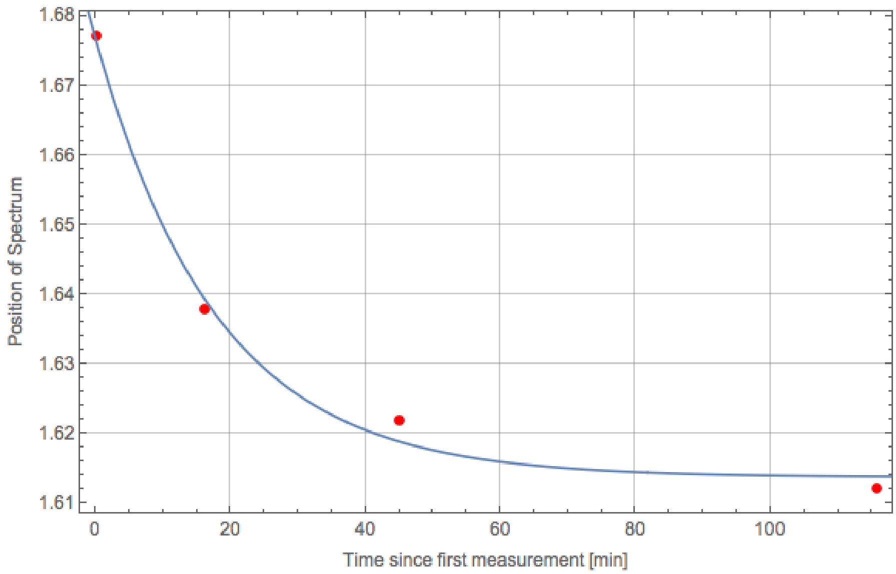

Figure 4.2: Drift of the spectrum through multiple consecutive measurements at $1010\,hPa$.

level. To consider this error all α values for each measurred pressure level are fitted to an exponential function. As an example figure 4.2 illustrates the drift of the data through multiple measurements all at approximately $1010\,hPa$. Even though the pressure level is highly stable the spectrum seams to drift to higher channel numbers. For the error estimation the difference between the offset of the fitted curve, which is the value that the exponential function aims towards, and the actual value used to define the spectrum position is taken.

This results in errors for both the pressure (relative to $1030\,hPa$) and the α values (also relative to the α value at $1030\,hPa$). Since linear fitting with errors in both the ordinate and abscissa coordinates is not implemented in Mathematica 11[1] (the software tool used for the evaluation of the spectrum data) a special fitting routine described in [22] is used to obtain a fitted model.

The resulting model can be seen in figure 4.3 which also indicates two different models where the input values where altered by $\pm 1\sigma$. This means that the real curve has a likelihood of 68% to lie within the area spanned by the dotted lines. The bars around each data point indicate the total error band in both the ordinate and the abscissa direction.

The obtained model $\alpha(\Delta p)$ illustrates the relative position α over the pressure difference Δp to the reference point:

[1] www.wolfram.com/mathematica

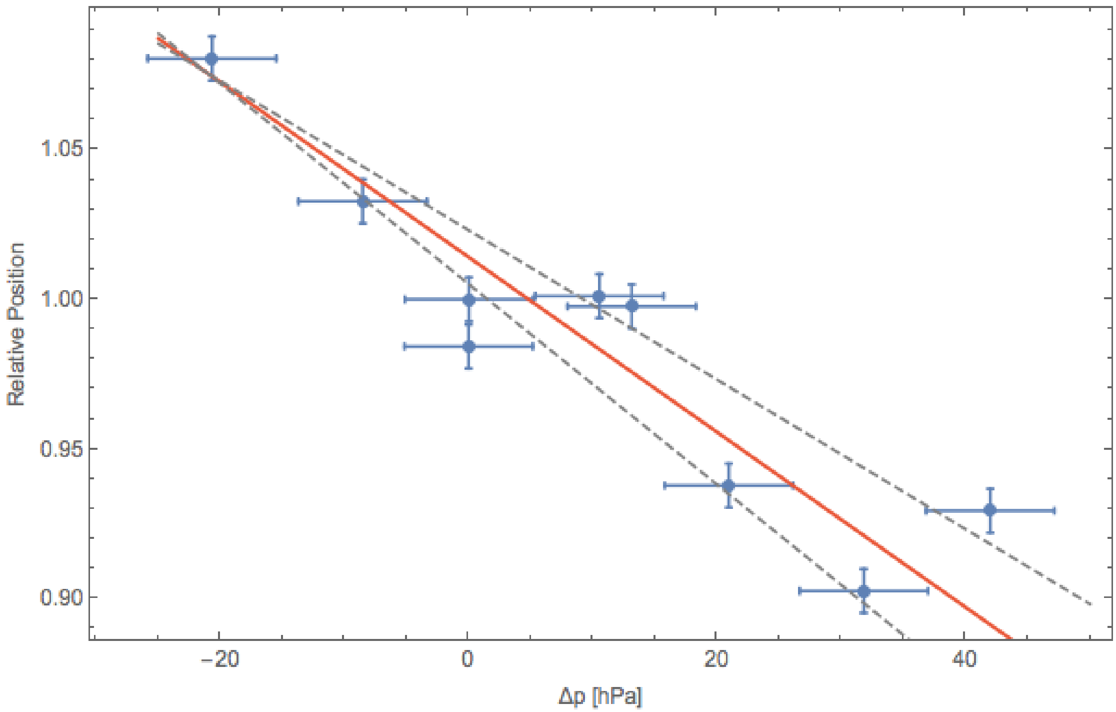

Figure 4.3: Overall model of the drift of spectrum data over pressure values, both relative to the reference point at $1030\,hPa$. Dotted lines show the same model with $\pm 1\sigma$.

$$\alpha(\Delta p) = (1.0140 \pm 0.0004) - (0.0029 \pm 0.0090) \cdot \Delta p \tag{4.1}$$

The linear fit has a χ^2 test statistic of 14.08 with 6 degrees of freedom and a significance level of 2.9%.

5 Conclusion

The aim of this thesis was to create a reliable software solution that integrates into the preexisting LabView environment. Through the design choices taken at an early stage it was possible to abstract the specific sensor parameters (e.g. I2C adress, number of sensors used, etc.) by using independent initialization files. For the first time it was possible to record the changing environmental parameters like gas pressure and flowrate inside the detector over a longer period of time. This allowed for a deeper understanding of the connection between mentioned parameters and the already known drift of the neutron spectrum.

Even though the obtained model has a poor significance level, the results can be used to estimate the effect that a changing air pressure has onto the spectrum position. To further increase the accuracy of the fit, more measurements should be done within the desired interval of pressure levels. It is very likely that the relation that describes the dependency of the spectrum drift on the gas pressure is only approximately linear within the reviewed pressure interval. Otherwise there would be pressure values where the spectrum would shift into negative channel numbers, which is not possible. Therefore it is expected that on a wider scale one would also need to consider ascending powers of the pressure value within the regression model. As the pressure inside the detector only slightly fluctuates around the value of the surrounding air pressure, the linear approximation for the dependency within the given interval is expected to be sufficient.

List of Figures

Bibliography

[1] S. K. Lamoreaux, R. Golub, and D. Richardson. *Ultra-cold neutrons.* CRC Press, 1991.

[2] P. J. Mohr, D. B. Newell, and B. N. Taylor. CODATA Recommended Values of the Fundamental Physical Constants: 2014, 2015.

[3] P. Callin and C. P. Burgess. Deviations from newton's law in supersymmetric large extra dimensions. 2005.

[4] A. N. Ivanov, G. Cronenberg, R. Höllwieser, T. Jenke, M. Pitschmann, M. Wellenzohn, and H. Abele. Exact Solution for Chameleon Field, Self–Coupled Through the Ratra–Peebles Potential with n = 1 and Confined Between Two Parallel Plates. 2016.

[5] J. Khoury and A. Weltman. Chameleon cosmology. *Physical Review D*, 2004.

[6] Nima Arkani-Hamed, Savas Dimopoulos, and Gia Dvali. Phenomenology, Astrophysics and Cosmology of Theories with Sub-Millimeter Dimensions and TeV Scale Quantum Gravity. 1998.

[7] T. Jenke et al. Ultracold neutron detectors based on 10B converters used in the qBounce experiments. In *Nuclear Instruments and Methods in Physics Research Section A: Accelerators, Spectrometers, Detectors and Associated Equipment 732*, 2013.

[8] H. Saul. Diplomarbeit, Technische Universität München. Weiterentwicklung des Detektor- und Auslesekonzepts für das Gravitationsexperiment qBounce, 2011.

[9] F. Atchison et al. Transmission of very slow neutrons through material foils and its influence on the design of ultracold neutron sources. *Nuclear Instruments and Methods in Physics Research A 608*, 2009.

[10] CR-110 charge sensitive preamplifier. `http://www.cremat.com/CR-110.pdf`. Accessed: 2016-12-09.

[11] Ortec 570 Amplifier. `www.ortec-online.com/download/570.pdf`. Accessed: 2016-11-30.

[12] quadADC. www.itech-instruments.com/quadADC_E.html. Accessed: 2016-11-30.

[13] Martin Thalhammer. Diplomarbeit, Technische Universität Wien. Optimierung der Detektorsignalverarbeitung des Gravitationsexperiments qBounce, 2013.

[14] Honeywell Zephyr Digital Airflow Sensors. http://sensing.honeywell.com/HAFBLF0200C2AX5-amplified-airflow-sensors.html. Accessed: 2016-12-09.

[15] P. T. Heistracher. Bachelorarbeit, Technische Universität Wien. Extension and Characterisation of the Neutron Detector within the qBounce Experiment, 2015.

[16] ASDX Series Silicon Pressure Sensors. https://sensing.honeywell.com/asdx-analog-ps-issue-9-008090-9-en-final-09sep09.pdf. Accessed: 2016-12-09.

[17] USB-I2C-Interface, Dokumentation und Anwendungsbeispiele. https://files.elv.com/Assets/Produkte/8/841/84123/Downloads/84123_usb_i2c_handbuch_v1_7.pdf. Accessed: 2016-12-09.

[18] LabVIEW. www.ni.com/labview/. Accessed: 2016-11-30.

[19] InterWinner. www.itech-instruments.com/InterWinner_E.html. Accessed: 2016-11-30.

[20] M. Klein. Doktorarbeit, Universität Heidelberg. Experimente zur Quantenmechanik mit ultrakalten Neutronen und Entwicklung eines neuen Detektors zum ortsaufgelösten Nachweis von thermischen Neutronen auf großen Flächen, 2000.

[21] Heavy Duty Pressure Transducers PX2 Series. www.mouser.com/ds/2/187/honeywell-sensing-px2-series-heavy-duty-pressure-t-740335.pdf. Accessed: 2017-06-20.

[22] Michael Krystek and Mathias Anton. A weighted total least-squares algorithm for fitting a straight line. *Measurement Science and Technology Volume 18, Number 11*, 2007.